POLYBENZENE AS A POSITIVE ELECTRODE IN AQUEOUS SECONDARY BATTERIES

ARNO PRUSS and FRITZ BECK*

University of Duisburg (GH), FB 6 - Elektrochemie, Lotharstrasse 1, 4100 Duisburg 1 (F R G)

(Received August 19, 1985)

Summary

Polybenzene (poly-*p*-phenylene, PPP) was chemically synthesized by the Kovacič method and electrodes fabricated with mixtures of 92.5 wt.% PPP and 7.5 wt.% carbon black by compression. The cyclic behaviour of these electrodes in 14 M H_2SO_4 under galvanostatic conditions ($j \cong 1$ mA cm^{-2}) has been investigated. From thin layer experiments, a maximum degree of insertion, $y_{max} = 0.17$, can be derived with reference to the aromatic unit $-C_6H_4-$, corresponding to an electrochemical charge density of about 50 A h kg^{-1}. The average discharge voltage is about 0.9 V *versus* SHE and the rate of self-discharge is as low as 1 μA cm^{-2}. Capacity loss upon cycling was due to shedding of active material and overoxidation of the host lattice. A comparison is made with graphite and other synthetic metals in aqueous and non-aqueous electrolytes

Zusammenfassung

Polybenzol (Poly-*p*-phenylen, PPP) wurde chemisch nach der Kovacič-Methode synthetisiert. Aus Mischungen von 92.5 Gew.% PPP mit 7.5 Gew.% Leitruss wurden Elektroden gepresst. Das zyklische Verhalten dieser Elektroden unter galvanostatischen Bedingungen ($j \cong 1$ mA cm^{-2}) wurde untersucht. Aus Dünnschichtversuchen kann ein maximaler Insertionsgrad von $y_{max} = 0.17$ (in bezug auf die Aromateneinheit $-C_6H_4-$) abgeleitet werden, was einem elektrochemischen Equivalent von etwa 50 A h kg^{-1} entspricht. Das durchschnittliche Entladepotential beträgt etwa 0.9 V gegen SHE. Die Selbstentladungsgeschwindigkeit ist mit 1 μA cm^{-2} sehr niedrig. Kapazitätsverluste beim Zyklisieren werden durch Ablosen der aktiven Masse und durch Überoxidation des Wirtsgitters verursacht. Vergleiche zum Graphit und zu anderen synthetischen Metallen in wässrigen und nichtwässrigen Elektrolyten werden durchgeführt.

*To whom correspondence should be addressed

0378-7753/85/$3 30

1. Introduction

The successful development of new batteries is predominantly a matter of material science. The "active masses" for electrochemical energy storage must optimally meet the "five Es", namely competitive *e*conomy, high *e*nergy densities, good electric as well as thermal energy *e*fficiencies, no *e*nvironmental hazards and last, but not least, reversible *e*lectrochemical behaviour, to realize high power densities and long cycle life. A new challenge arose at the end of the 1970s with the conducting polymers, based initially on polyacetylene [1 - 3]. Structural alternatives such as poly-*p*-phenylene PPP ("polybenzene") [4, 5], polypyrrole [6] and polythiophene [7] became interesting owing to their improved stability. Upon cycling, these polymers, with conjugated double bonds, act as host lattices for anions or cations which are electrochemically inserted or removed They can be regarded as ideal battery electrodes. In the case of polybenzene, the overall reaction for an insertion compound of the acceptor type can be expressed as

$$(-C_6H_4-)_x + xyA^- + \nu xyHA \underset{\text{disch}}{\overset{\text{ch}}{\rightleftharpoons}} [(-C_6H_4-)^{y+} \cdot yA^- \cdot \nu yHA]_x + xye^- \quad (1)$$

where x is the degree of polymerization, y the degree of insertion of anion A^-, and ν the stoichiometric number for solvate acid HA.

Broad experience with other insertion electrodes, *e g.* inorganic compounds such as MnO_2 [8], V_6O_{13} [9] or TiS_2 [10], and graphite [11], is of some benefit While in the former case the stoichiometric degree of insertion is high (typically $y = 100\%$) and reversibility is limited, the situation in the case of graphite intercalation compounds is quite the opposite low y (2% - 4%) is linked with extremely good cyclic behaviour, according to Fuji's [12, 13] and our own [14 - 17] investigations. These earlier findings serve as landmarks for new developments, and it is hoped to combine the high y of inorganic systems and the high stability of graphite with the intrinsic low equivalent weights of the new systems.

In most cases, the new polymers have been used in aprotic electrolytes, allowing the application of lithium negatives. However, the behaviour of this metal electrode is poor on cycling in these electrolytes. More recently, aqueous electrolytes have been shown to be applicable for polyacetylene [18 - 20] and for polybenzene [21 - 23]. Only for polybenzene (and polythiophene), however, but not for polyacetylene (and polypyrrole), is the potential sufficiently positive for practical use. We have extended our former voltammetric investigations of PPP [22, 23], synthesized chemically by the Kovacic method [24, 25], to galvanostatic cycling experiments with single electrodes in aqueous sulphuric acid, including thin layer electrodes, in order to simulate battery conditions

2. Experimental

The chemical oxidation of benzene under mild conditions ($CuCl_2$ as an oxidant, $AlCl_3$ as a Friedel–Crafts catalyst, reaction temperature 0 - 80 °C)

yields poly-*p*-phenylene (PPP) as a light, brown powder, insoluble in all solvents and infusable [24, 25]. We applied Kovacic *polymerization* under standard conditions, as described before [22]. Elementary analysis revealed a lower concentration of H, −5% to −7% below the theoretical composition $(C_6H_4)_x$, in agreement with Kovacic and Kyriakis [24]. Linkage in the *p*-position dominates absolutely, unlike products with $FeCl_3$ [22, 24], or the anodically deposited layers on Pt from aqueous H_2F_2 [21, 26].

The dry PPP powder was mixed with 7.5 wt.% soot (carbon black) Corax L® from the Degussa Company. Pellets were fabricated from this mixture in a mould of steel at 570 MPa. They were 17 mm in diameter, 1 - 2 mm thick and had a resistivity of 300 Ω cm [22]. Analogous mixtures with 10% Ketjenblack EC® have a resistivity of 200 Ω cm as a pellet. The so-called *pellet electrodes* were made by mounting these discs — after gently roughening both sides with fine carborundum paper — in an electrode holder described in ref. 22. The free area exposed to the electrolyte was reduced to 1.3 cm^2 In the course of the electrochemical experiments, only a surface layer of about 0.1 mm thick participated in the electrochemical conversion.

In order to achieve total conversion of the PPP material, thin layer electrodes were made by the following procedures

Pressed thin layer (PTL) electrodes were made by application of the above-mentioned mixtures, PPP/carbon black, onto base electrodes of Pt mesh (400 cm^{-2}), p = 50 MPa, 20 °C. The final thickness was about 100 μm. Etched titanium expanded sheet, 12 holes/cm^2, was also suitable. A stand at open-circuit voltage, however, led to activation of the Ti within a few minutes. Nevertheless, under cycling conditions, the Ti can be regarded as virtually inert.

Dipped thin layer (DTL) electrodes were started from a typical dispersion of 750 mg PPP and 250 mg Ketjenblack EC® in 10 ml tetrahydrofuran, containing 100 mg of PVC (Vinoflex S 6815, BASF Co.). After three dips of the sheet electrode, made of 0.1 mm smooth Pt, with intermediate drying and a final drying stage at 80 °C, a black layer of reasonable adherence and a thickness of a few μm was formed.

Counter-electrodes were made from CPP (80 wt.% purified natural graphite and 20 wt.% polypropylene). The *reference electrode* was always Hg/Hg–I-sulphate in 1 M H_2SO_4. Potentials are denoted as U_s and are U_s + 674 mV *versus* SHE.

The *electrolyte* was 14 M H_2SO_4, made from 97% H_2SO_4 p.a from Merck and distilled water, as a compromise between the poor electrochemical behaviour of PPP in more diluted (< 10 M) acid [22] and the chemical attack of metals (as possible candidates for negative electrodes) in concentrated (18.3 M) H_2SO_4 All measurements were performed in unstirred electrolyte at 20 °C

The PPP electrodes were galvanostatically cycled using voltage limits. The charge and rest times [27] could be preset between 10^{-2} and 10^5 s and the charge/discharge curves were plotted on an x/t recorder.

3. Results and discussion

3.1. Typical galvanostatic potential/time behaviour

A typical cycling curve with a PTL electrode is represented in Fig. 1. The average charging potential is $U_s \cong 0.3$ V, in agreement with the potential at which a steep rise of the anodic current/voltage curve occurs in 14 M H_2SO_4 [22]. Discharge potentials are shifted to more negative values as is also indicated in the current/voltage curves. The first charging curve (up to the preset end-potential of $U_s = 0.45$ V) is much longer than all the following ones. We presumed that this could be due to anodic oxidation of low molecular weight impurities present in the polymer. Control experiments with PPP, purified in two steps ((1) boiling with dilute HCl, (2) 24 h boiling with toluene), however, did not change this general behaviour at all. It therefore seems that some formation process of the compressed PPP/carbon black mixture is responsible. Carbon black alone has no electrochemical activity in this potential region [22]. The capacity of the electrode decreases during the following cycles, while the current efficiency tends to become virtually constant (see §3.3). After some formation, the occurrence of steps in the charging curve become obvious

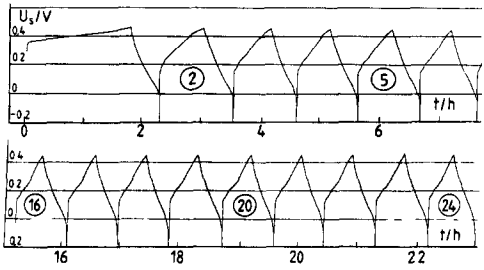

Fig 1 Cyclic galvanostatic charge/discharge curves of a PTL electrode on Pt mesh 92 5 wt % PPP, 7 5 wt.% Corax L®, m = 49 mg, i = 3 mA, area $A \sim 1$ 5 cm^2 (single side) Charging up to U_s = 0 45 V, deep discharge down to U_s = −0 2 V, electrolyte = 14 M H_2SO_4

The overall behaviour does not change with the DTL electrodes, as demonstrated by the example in Fig. 2. The appreciably smaller capacity is compensated experimentally by the lower current density. Ketjenblack EC®, which was used in this case as carbon black, showed some increase of basic current in comparison to Corax L®.

3.2. Evaluation of y_{max}

In our previous work [22, 23], we used pellet electrodes of 1 - 2 mm thickness exclusively. After some voltammetric formation cycles, a surface layer of about 0.1 mm took part in the electrochemical conversion. The maximum degree of insertion, y_{max}, could only be determined arbitrarily. With our thin layer electrodes, we are now able to derive more reliable values.

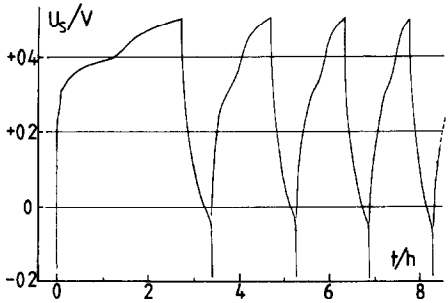

Fig 2 Cyclic galvanostatic charge/discharge curves of a DTL electrode on Pt sheet m = 2 4 mg (68 wt.% PPP, 23 wt % Ketjenblack EC®, 9 wt % PVC from THF solution), i = 0 2 mA, total area $A \sim 4$ cm^2 Charging up to U_S = 0 51 V, deep discharge down to U_S = —0 2 V, electrolyte = 14 M H_2SO_4

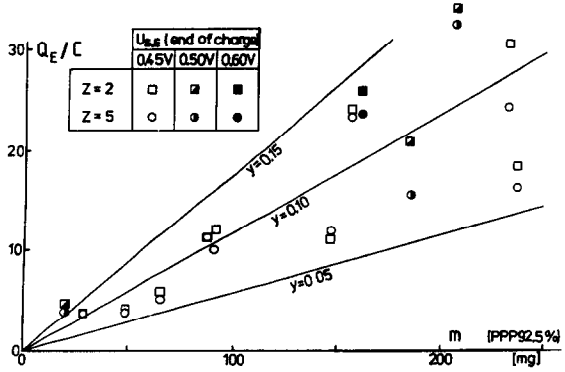

Fig 3 Evaluation of discharge capacity Q_E *vs* mass m of PPP (as a 92 5 wt % mixture with 7 5 wt % Corax L®) with a PTL electrode for y_{max} Results after two and five cycles for three different end-potentials of charging, $U_{S,E}$ $U_{s,disch}$ = —0 2 V, electrolyte = 14 M H_2SO_4

Figure 3 represents a plot of discharge capacity Q_E against mass of 92.5 wt.% PPP in PTL electrodes cycled according to Fig. 1. The end-potential of charging, $U_{S,E}$, was the experimental parameter which was changed. Theoretical lines for three degrees of insertion y are drawn in addition. y refers to one benzene ring and is defined as

$$y = \frac{Q_E M_{C_6H_4}}{Fm(\text{PPP}, 100\%)} \tag{2}$$

It can be seen from Fig 3 that y_{max} is about 0.15, obtainable at higher levels of $U_{S,E}$.

These findings are confirmed with the even thinner DTL electrodes (see Fig. 4). The average value of y_{max} corresponds roughly to $y_{max} \cong 1/6$, which means that every sixth benzene ring is oxidized to the radical cation.

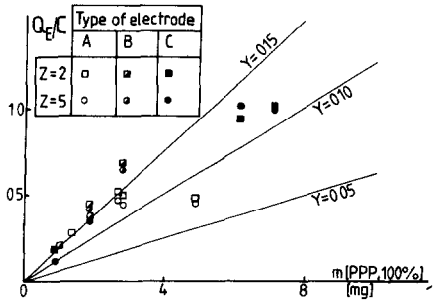

Fig 4 Evaluation of discharge capacity Q_E *vs* mass of PPP contained in various DTL electrodes A, B, C for y_{max} Results after two and five cycles for the following systems A, dispersion of 750 mg PPP and 250 mg Ketjenblack in 10 ml dichloroethane with 50 mg epoxy resin and 50 mg hardener dissolved in it, composition of solid layer 68 wt % PPP/23 wt % Ketjenblack/9 wt % binder B, dispersion of 750 mg PPP and 250 mg Ketjenblack in 10 ml THF with 100 mg PVC dissolved in it, composition of solid layer 68 wt % PPP/23 wt % Ketjenblack/9 wt % PVC C, dispersion of 1 0 g of a dry mixture containing 90 wt % PPP and 10 wt % Ketjenblack in 10 ml THF with 100 mg PVC dissolved in it, composition of solid layer 82 wt % PPP/9 wt % Ketjenblack/9 wt % PVC End-potential of charging $U_{S,E}$ = 0 51 V, $U_{s,disch}$ = −0 2 V, electrolyte = 14 M H_2SO_4

3.3. Formation and extended cycling behaviour

The degree of insertion y evaluated from the discharge capacity Q_E, and the current efficiency α calculated according to

$$\alpha = Q_E/Q_{ch} \tag{3}$$

as a function of cycle number Z are shown in Fig. 5 for two characteristic galvanostatic cycling experiments. Run No. 1 (with Pt as the base electrode) exhibits a continuous slow loss of discharge capacity upon cycling. This can be ascribed to overoxidation of the host lattice According to our very slow cyclic voltammetric measurements [28], this process starts as $U_s \sim 0.4$ V and leads to the introduction of carboxylic groups accompanied by cleavage of C—C bonds. Experiment No. 2 was performed under more severe conditions (end-potential of charging $U_{S,E}$ = 0.60 V), and the initial loss of capacity is even more pronounced. Presumably, a loss of ohmic contact of active mass

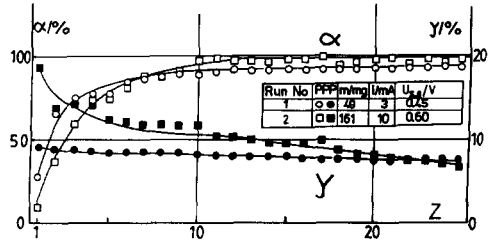

Fig 5 Formation behaviour for two galvanostatic cycling experiments with PTL electrodes (92 5 wt % PPP/7.5 wt.% Corax L®) under deep discharge No 1 used Pt as the base electrode (*cf* Fig 1), No 2 was performed with Ti as the base metal $U_{s,disch}$ = −0 2 V in both cases, electrolyte = 14 M H_2SO_4

is also involved in this case. After about ten formation cycles a quasi steady state is reached in both cases, and an α of 99% or even higher allows cycle numbers of 100 or more. We have previously [27] found an analogous increase of α in the course of galvanostatic cycling with polypropylene-bound graphite. An improvement of the electrode in terms of a compressed sandwich with porous separators to prevent active mass shedding seems possible.

We fabricated thin (0.05 mm) sheets of 30% - 40% PPP, 7% - 12% carbon black and 63% - 48% polyethylene or PVC (mixed in a plastic kneader then hot pressed at 27 MPa and 150 °C between Al foils). These sheets could not be operated as free-standing foil electrodes as poor conduction and formation behaviour lead to poor y values. The resistivity was much higher than with layers which had been homogenized and pressed at room temperature, with or without a binder ($\cong 10^8\ \Omega$ cm compared with $\cong 10^3\ \Omega$ cm). In this case, it was necessary to raise the carbon black concentration to 20 wt.% to achieve a resistivity of $10^3\ \Omega$ cm.

3.4. Partial cycling

A cycling experiment was initiated with a PTL electrode in rough analogy to that represented in Fig 1. After two complete cycles and a third charge, the discharge was stopped after the removal of about 10% of the last discharge capacity, and the same charge was introduced again into the system. According to Fig. 6, these partial discharge cycles could be repeated 57 times before the lowest discharge potential reached the original low level of complete discharge Assuming that the limitation of the partial cycling process to Z' cycles is due to an unbalanced charging process, a partial charge $\alpha_p\ \Delta Q$ is introduced instead of ΔQ with each partial charge, but ΔQ is removed The total inventory Q_0 is exhausted after Z' cycles, and α_p can be calculated according to [29]

$$\alpha_p = 1 - Q_0/\Delta Q\ Z' \qquad (4)$$

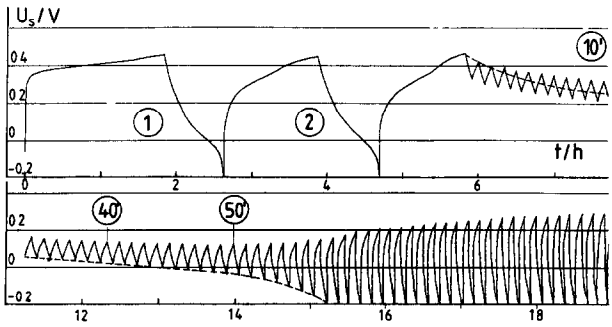

Fig 6 Galvanostatic partial cycling experiment with a PTL electrode on Pt mesh 92 5 wt % PPP and 7 5 wt % Corax L®, m = 94 mg, i = 5 mA, $U_{S,E}$ = 0 45 V, Q_{disch} = 14 6 C (second cycle), ΔQ = 1 5 C (partial cycling) The broken line indicates the last discharge curve, expanded to the time of the partial cycling experiment, electrolyte = 14 M H_2SO_4

With the data of the experiment shown in Fig. 6, $\alpha_p = 0.83$, which is lower than $\alpha = 0.93$ following from the deep discharge cycles represented in Fig 1.

3.5. Self-discharge

Self-discharge of a charged electrode standing at open-circuit potential (ocp) has been investigated as it is an important battery electrode parameter. Figure 7 shows the ocp/time curve. After an initial decrease, due to flattening of the concentration profiles, a quasi steady state potential was maintained at $U_s \cong 0.2$ V for a long time. Discharge of the residual charge after $\tau = 1079$ (2663) hours for run No. 1 (2) revealed the presence of $\beta = 55\%$ (9%) of the initial charge (in terms of Q_E of the last deep discharge). From these data, the *average* corrosion current density j_{corr} can be calculated from

$$j_{corr} = Q_E(1 - \beta)/\tau \tag{5}$$

The results are 1.4 (1.1) μA cm^{-2}, demonstrating a rather low rate of self-discharge in 14 M H_2SO_4. For these experiments, the pellet electrode was used so as to exclude any localized cell action with the base electrode material.

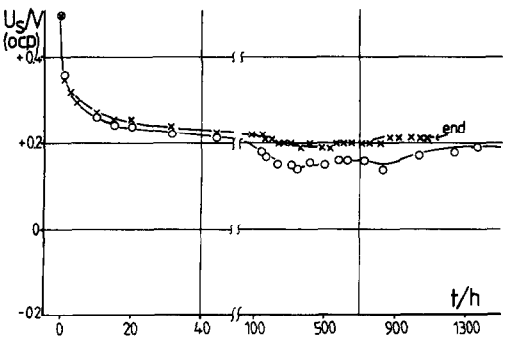

Fig 7 Potential (open-circuit)/time curves of two parallel runs for evaluation of the rate of self-discharge Pellet electrode, 92 5 wt % PPP/7 5 wt % Corax L®. Current density j for seven complete cycles of formation = 0 5 mA cm^{-2} Q_{disch} of last deep discharge = 12 2 C Residual discharge β for run 1 after 1079 h = 55%, for run 2 after 2663 h = 9% Electrolyte = 14 M H_2SO_4

Confirmation of these findings was obtained by systematic variation of the rest time (stand at open-circuit voltage) τ. Increasing τ decreased the residual discharge capacity Q_{rel}. Figure 8 shows two plots of current efficiency α_{res} against τ for two different electrolytes. α_{res} is defined as

$$\alpha_{res} = Q_{rel}/Q_{ch} \tag{6}$$

where Q_{ch} is the last charge capacity. From the slope of this curve, the corrosion current density can be obtained [27] according to

$$j_{corr} = \Delta\alpha_{res} Q_{ch}/\Delta\tau \tag{7}$$

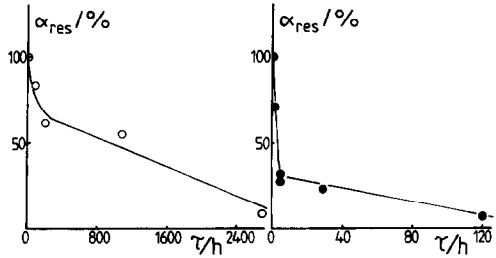

(a) (b)

Fig 8 Residual discharge capacity evaluation of a pellet electrode (92 5 wt.% PPP, 7 5 wt % Corax L®) in electrolyte (a) 14 M H_2SO_4 and (b) 6 M H_2SO_4 after an open-circuit potential stand of time τ Discharge current density = 1 5 mA cm^{-2} Formation (ten cycles) and last charge are both in 14 M H_2SO_4 at 1 5 mA cm^{-2} ($U_{S,E}$ = 0 51 V) The ordinate α_{res} is defined in the text

The initial slope is greater than the steady state slope. This is due to a high initial surface concentration of insertion compound. In 14 M (6 M) H_2SO_4, an initial j_{corr} of 35 (350) μA cm^{-2} is calculated within the first 100 (5) hours. The quasi steady state value is 0.6 (4.3) μA cm^{-2}. The values calculated from eqn. (5) are an average of both regimes.

3.6. Formation of the pellet electrode

Galvanostatic cycling experiments were performed to gain further insight into the complex processes occurring in the compressed PPP/carbon black mixtures under current drain. According to Fig 9, Q_E increases linearly with time due to a formation process, which reflects successive penetrations of the active zone into the pellet to a depth of 1 - 2 mm. This formation effect was much less pronounced in our previous cycling experiments with pellet electrodes under slow cyclo-voltammetric conditions [22, 23]. This can be readily explained in terms of higher current densities at more positive potentials for much longer periods in the case of galvanostatic cycling. α remains at a relatively low level (60%) as that part of each new cycle is run under "initial conditions" (see Fig. 5). After 25 cycles, Q_E is

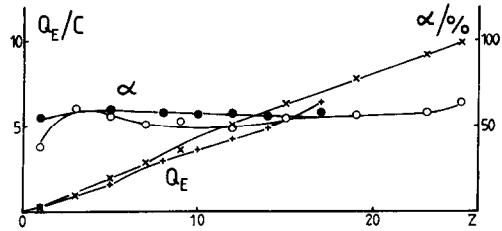

Fig 9 Galvanostatic cycling of a pellet electrode, 92 5 wt % PPP/7 5 wt % Corax L® $j_{ch} = j_E \cong 1$ mA cm^{-2}, $U_{S,E}$ = 0 51 V, deep discharge to U_s = −0 2 V Plot of discharge capacity Q_E (×, +) and current efficiency α (○, ●) *vs* cycle number Z for two independent runs Electrolyte = 14 M H_2SO_4

about 10 C, corresponding to a depth of penetration d of about 0.3 mm, assuming total conversion up to y_{max} Penetration values observed at the end of the experiment were even higher by a factor of 2 - 3.

4. Conclusions

Our results obtained with thin layer PPP electrodes allow reliable calculation of the maximum degree of insertion y_{max}. From Figs. 3 and 4, y_{max} is slightly above 15%. We conclude from this that every sixth benzene ring can be oxidized to a radical cation site. The macro radical cation is virtually stable, even in aqueous electrolytes, as shown by the cycling experiments. The positive charge is compensated by the insertion of anions. From our previous findings [22, 23], a co-insertion of two molecules of solvate acid per anion is derived. The PPP host lattice contains stacked chains of PPP molecules. The above-mentioned stoichiometry leads, qualitatively, to a distribution of anions and solvate molecules, as outlined in Fig. 10. This is similar to the *structure* of graphite hydrogen sulfate, shown for comparison. The most important difference is the direction of the main electronic conductivity: along the c-axis in PPP (through the stack perpendicular to the chains), but perpendicular to the c-axis in graphite (along the planes). y_{max} is important for battery applications, as it governs the maximum *electrochemical equivalent*

$$m_e = \frac{y_{max} F}{M_B + y_{max} M_A} \tag{8}$$

where M_B and M_A are the molecular weights of the host lattice unit and the anion, respectively. This equation does not consider co-insertion of solvate acid or solvent molecules.

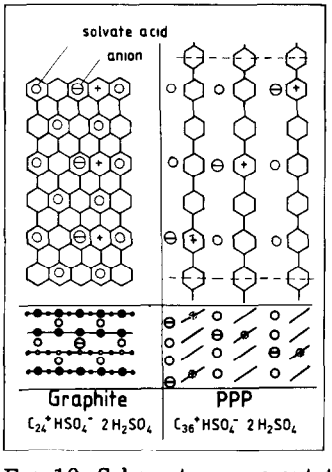

Fig 10 Schematic representation of the structure of a graphite intercalation compound and the poly-*p*-phenylene insertion compound of acceptor type

TABLE 1

Battery positives from graphite and conducting polymers in aqueous (a) and non-aqueous (na) electrolytes [22]

Polymer host lattice	Electrolyte	C_1 unit	M (g) (C_1 unit)	y_{max} (C_1 unit)	m_e (A h kg^{-1})	U_H (V)
Graphite	a	C	12	0 021	39 9	1 7
	na	C	12	0 042	69 1	2 0
PPP	a	$CH_{0.67}$	12 7	0 028	48 4	1 3
	na [5]	$CH_{0\ 67}$	12 7	0 08	103 6	1 6
Polyacetylene	a [20]	CH	13	0 045	68.9	0 6
	na	CH	13	0 1	116 5	0 7
Polypyrrole	na	$CH_{0\ 75}N_{0.25}$	16 3	0 09	95 3	0 3
Polythiophene	na	$CH_{0\ 50}S_{0\ 25}$	18 5	0 13	110 6	1 0

Table 1 compares graphite and various polymer materials for aqueous and non-aqueous electrolytes. To improve comparability, all values refer to a C_1 unit. M_A is assumed to be 100.

Table 1 shows that the specific capacity m_e of PPP is slightly superior to that of graphite, but other conducting polymers show appreciably higher values of y_{max} On the other hand, the *potential level* is most positive for PPP, as shown in the last column.

The addition of about 10 wt.% *carbon black* proved to be suitable to attain an appropriate conductivity. The same effect has been reported previously for polyacetylene [30].

Galvanostatic cycling was applied in the region of 1 mA cm^{-2} The *formation* of the electrodes was stronger than in our former slow cyclovoltammetric experiments [22, 23]. The *loss of capacity* is due to shedding of active mass in the initial stages. Overoxidation of the PPP host lattice plays an additional role. The *stability* is superior to that of polyacetylene, but less than that of graphite. The *cost* of PPP material is higher than for natural graphite, but synthetic polymers have the great advantage that they can be fabricated on an industrial scale, starting from well-defined monomers.

Acknowledgements

Financial support of this work by the Deutsche Forschungsgemeinschaft is gratefully acknowledged. The authors wish to thank Akzo AG, Düren, and Degussa AG, Frankfurt, for providing the carbon black, as well as BASF AG, Ludwigshafen, and Hoechst AG, Frankfurt, for the polyethylene and PVC (powder)

List of symbols

F	Faraday constant
j	Current density
j_{corr}	Corrosion current density
m	Mass
M	Molecular mass
Q_{ch}	Charge capacity
Q_E	Discharge capacity
Q_{rel}	Residual capacity
Q_0	Initial capacity
ΔQ	Partial capacity
U	Voltage
U_H	Potential *versus* SHE
U_s	Potential *versus* $Hg/Hg_2SO_4/1$ M H_2SO_4 reference electrode
x	Degree of polymerization
y	Degree of insertion
y_{max}	Maximum degree of insertion
Z	Cycle number, number of cycles
α	Current efficiency (A h efficiency)
α_p	Current efficiency for partial cycles
ν	Stoichiometric number for solvate acid HA
τ	Time constant, rest time

References

1 A G. McDiarmid and A. J Heeger, *Synth Met*, *1* (1979) 101
2 P J Nigrey, D McInnes, D P Nairns, A G McDiarmid and A J Heeger, *J Electrochem Soc*, *128* (1981) 1651, see also A G McDiarmid *et al*, Univ Patent Inc, *Eur Patent 36,118*, 1980
3 R B Seymour (ed), *Conductive Polymers*, Plenum Press, New York, 1981
4 D M Ivory, G G Miller, J M Sowa, L W Shacklette, R R Chance and R. H Baughman, *J Chem. Phys*, *71* (1979) 1506
5 L M Shacklette, R L Elsenbaumer, R C Chance, J M. Sowa, D M Ivory, G G. Miller and R H Baughman, *J Chem Soc*, *Chem Commun*, (1982) 361.
6 A F Diaz, *Chem Scr*, *17* (1981) 145
7 G Tourillon and F Garnier, *J Electroanal Chem Interfacial Electrochem*, *135* (1982) 173
8 A Kozawa and R A Powers, *J Electrochem Soc*, *113* (1966) 870, see also J E Colemann, *Trans Electrochem. Soc*, *90* (1946) 545
9 A Hooper and B C Tofield, *J Power Sources*, *11* (1984) 33
10 M St Whittingham, *J Electrochem. Soc*, *123* (1976) 315
11 W Rudorff and U. Hofmann, *Z Anorg Allg Chem*, *238* (1938) 1
12 R Fujii, *Denki Kagaku*, *40* (1972) 380, 705
13 R Fujii, *Rep 353*, Gov Ind Res Inst Osaka, 1978, p 1
14 F Beck, H. Junge and H Krohn, *Electrochim Acta*, *26* (1981) 799, F Beck, W Kaiser and H Krohn, *Angew Chem Suppl*, (1982) 57
15 F Beck and H Krohn, *DECHEMA-Monogr*, *92* (1982) 57

16 F Beck, *Elektrotechniek (Netherlands), 61* (1983) 178
17 F Beck and H Krohn, *J Power Sources, 12* (1984) 9
18 A Guiseppi-Elie and G E Wnek, *J Chem Soc, Chem Commun*, (1983) 63
19 A. G McDiarmid and R J Mammone, *Eur Patent 131,829*, 1983
20 K. H Dietz and F Beck, *J Appl Electrochem, 15* (1985) 159
21 I Rubinstein, *J Electrochem Soc, 130* (1983) 1506
22 F Beck and A Pruss, *Electrochim. Acta, 28* (1983) 1847
23 A Pruss and F Beck, *J Electroanal Chem Interfacial Electrochem., 172* (1984) 281
24 P Kovacič and A Kyriakis, *J Am Chem Soc, 85* (1963) 454, *Tetrahedron Lett*, (1962) 467
25 P Kovacič and J Oziomek, *J Org Chem, 29* (1964) 11, *Macromol Synth, 2* (1966) 23, M B Jones, P Kovacič and D Lanska, *J Polym Sci, Polym Chem Ed, 19* (1981) 89
26 I. Rubinstein, *J Polym. Sci, Polym. Chem Ed, 21* (1983) 3035
27 F Beck, H Krohn and W Kaiser, *J Appl Electrochem., 12* (1982) 505
28 F Beck and A Pruss, unpublished
29 F. Beck, H Krohn and W Kaiser, *J Electroanal Chem Interfacial Electrochem, 165* (1984) 93
30 R Th Gray, Rohm and Haas Co, *Eur Patent 50,441*, 1981